Clinical Oral Investigations
https://doi.org/10.1007/s00784-018-2496-9

ORIGINAL ARTICLE

Metabolomics profiling of cleidocranial dysplasia

Zhaoqiang Zhang[1] · Kefeng Li[2] · Mengdie Yan[3,4] · Qiuping Lin[3] · Jiahong Lv[3] · Ping Zhu[5] · Yue Xu[3]

Received: 11 January 2018 / Accepted: 24 May 2018

Abstract

Objectives Cleidocranial dysplasia (CCD) is a rare autosomal-dominantly inherited skeletal dysplasia that is predominantly associated with heterozygous mutations of *RUNX2*. However, no information is available regarding metabolic changes associated with CCD at present.

Materials and methods We analyzed members of a CCD family and checked for mutations in the *RUNX2* coding sequence using the nucleotide BLAST program. The 3D protein structure of mutant RUNX2 was predicted by I-TASSER. Finally, we analyzed metabolites extracted from plasma using LC-MS/MS.

Results We identified a novel mutation (c.1061insT) that generates a premature termination in the *RUNX2* coding region, which, based on protein structure prediction models, likely alters the protein's function. Interestingly, metabolomics profiling indicated that 30 metabolites belonging to 13 metabolic pathways were significantly changed in the CCD patients compared to normal controls.

Conclusions The results highlight interesting correlations between a *RUNX2* mutation, metabolic changes, and the clinical features in a family with CCD. The results also contribute to our understanding of the pathogenetic processes underlying this rare disorder.

Clinical relevance This study provides the first metabolomics profiling in CCD patients, expands our insights into the pathogenesis of the disorder, may help in diagnostics and its refinements, and may lead to novel therapeutic approaches to CCD.

Keywords CCD · Metabolic changes · RUNX2 · Mutation · Patients · Protein structure

Introduction

Cleidocranial dysplasia (CCD, OMIM #11 9600) is a rare autosomal-dominantly inherited skeletal dysplasia with varying clinical symptoms ranging from isolated dental abnormalities to the complete absence of clavicles or ossification of parietal bones. Classic clinical manifestations include delayed closure of cranial sutures, congenital clavicular hypoplasia, open fontanelle, short stature, and dental abnormalities; manifestations may also extend to short distal phalanges and vertebral abnormalities. Among these phenotypes, one of the main features is disturbed dentition including the delayed eruption of permanent teeth and supernumerary teeth [1–3].

It is generally believed that mutations of the osteoblast-specific transcription factor gene (runt-related transcription factor-2, *RUNX2*) are responsible for these phenotypes [3, 4]. The *RUNX2* gene, located on chromosome 6p21, plays an important role in skeletal development by regulating osteoblast function and chondrocyte maturation [5, 6]. *RUNX2* has eight coding exons but gives rise to a variety of distinct transcripts that include or lack specific exons. The full-length protein contains a glutamine and alanine (Q/A) repeat domain, a runt domain, a C-terminal proline–serine–threonine (PST)-rich domain, and a VWRPY motif [7]. Both the Q/A and PST domains serve as transcriptional activation domains. Recent studies have revealed a number of direct or indirect target genes of *RUNX2* including matrix metalloproteinase 13 (*MMP13*), SMAD family member 3 (*SMAD3*), *P21*, and

✉ Yue Xu
kou9315@hotmail.com

1 Department of Oral and Maxillofacial Surgery, Stomatological Hospital, Southern Medical University, No. 366, South of Jiangnan Road, Guangzhou, Guangdong 510280, People's Republic of China

2 San Diego (UCSD) School of Medicine, University of California, 214 Dickinson St., Bldg CTF, Room C111, San Diego, CA 92103-8467, USA

3 Department of Orthodontics, Guanghua School of Stomatology, Hospital of Stomatology, Sun Yat-sen University, No. 56 Lingyuanxi Road, Yuexiu District, Guangzhou, Guangdong 510055, People's Republic of China

4 Present address: Department of Orthodontics, Stomatological Hospital, Southern Medical University, No. 366, South of Jiangnan Road, Guangzhou, Guangdong 510280, People's Republic of China

5 Department of Oral and Maxillafacial Surgery, Guanghua School of Stomatology, Hospital of Stomatology, Sun Yat-sen University, No. 56 Lingyuanxi Road, Yuexiu District, Guangzhou, Guangdong 510055, People's Republic of China

Table 1 Primers used in PCR

Exon	Sense	Antisense
2	CCACCGAGACCAAC AGAGTC	TCTTTTACTGTTTTCATATC CTCACC
3	CGGCAGTCGGCCTCATCAAA	GCTCGCAGTGCAAGAGTGGGTAC
4	TGGCATCACAACCCATACAC	TGCTCACACCCAGTGAAATTAG
5	GTCTTTGTTTCATTGCCTCC	CAAAGTCCACAAAGACACTATGG
6	TCCTTGGCTTAAACTCCCAG	AATAAGCCGCTTCACAGCTC
7	TAAGGCCTGAAAGGATGGG	ATTTGCCAGTTGTCATTCCC
8	CTCTCTGTCTACCCCTCCCC	AAATGCAAGGGTTAAGTGCC
9	GCTTGCTGTTCCTTTATGGG	CTACCCTCTTATGGCTGCAAG

vascular endothelial growth factor (*VEGF*) [8–13]. These target genes influence not only signaling networks in osteoblasts but more generally intracellular transport, cell cycle parameters, cytokine production, inflammatory responses, hormone biosynthesis, and metabolism [14–17]. Hence, mutations of *RUNX2* in CCD patients likely affect multiple target genes and the corresponding biological processes.

With the recent breakthrough in metabolomics technology, this technology is increasingly applied in medicine not only to acquire fundamental knowledge on pathogenesis but also to identify novel biomarkers and to study the effects of drug therapy [18]. To our knowledge, however, no information is available on the metabolic pathways for CCD patients.

The current study identified a novel *RUNX2* mutation in a CCD family and assessed metabolic changes in affected members of this family. Our research may provide further insights into the pathogenesis of CCD and could help in developing novel diagnostic and therapeutic approaches.

Materials and methods

Patients

The initial proband of the recruited family was a 24-year-old female referred to the Department of Orthodontics, Hospital of Stomatology, Sun Yat-sen University, who presented with a major complaint regarding unerupted teeth and a desire for orthodontic treatment. The family history showed that her maternal grandmother, her mother, an uncle, and a cousin also showed delayed eruption of their permanent teeth, while other relatives were free of any skeletal or dental abnormalities. All patients were examined clinically but only some of them radiologically due to restricted local medical services or a patient's lack of consent to be examined radiologically.

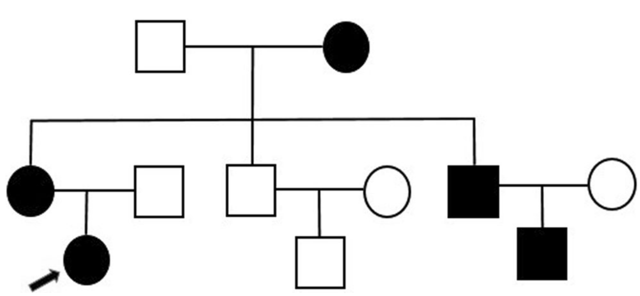

Fig. 1 The pedigree of the CCD family. Black arrow indicates the proband; squares indicate males and circles indicate females; black indicates CCD patients and white indicates unaffected family members

Mutational analysis of *RUNX2* and 3D protein structure predictions

Genomic DNA was extracted from the peripheral blood of the patients and normal controls using the QIAamp DNA Blood Midi kit (Qiagen, Valencia, CA, USA) according to the manufacturer's instruction. OD_{260}/OD_{280} of genomic DNA was analyzed by spectrophotometry to assess DNA purity and concentration. The eight coding exons of the *RUNX2* gene were amplified by polymerase chain reaction (PCR) using the primers indicated in Table 1. Reference sequences and the number of coding exons refer to GenBank accession number NM_001024630. PCR products were purified and subjected to direct sequencing using an ABI 3730 XL (automatic sequencer, Hilden, Germany) according to the manufacturer's protocols. Mutations were analyzed using the nucleotide BLAST program (http://blast.ncbi.nlm.nih.gov/). The 3D protein structures of wild-type and mutant *RUNX2* as well as isolated wild-type and mutant exon 8 were predicted by I-TASSER (http://zhanglab.ccmb.med.umich.edu/I-TASSER/).

Extraction of metabolites from plasma

Peripheral blood was drawn from five CCD patients and three normal controls. Plasma was cleared by centrifugation at 600×*g* for 5 min at −20 °C. Typically, 100 μl of plasma was mixed with 400 μl of 100% methanol containing ^{13}C-labeled standards. The mixtures were vortexed for 30 s and incubated on ice for 10 min. The mixtures were then centrifuged at 15,000 rpm for 10 min at 4 °C. The resulting supernatants

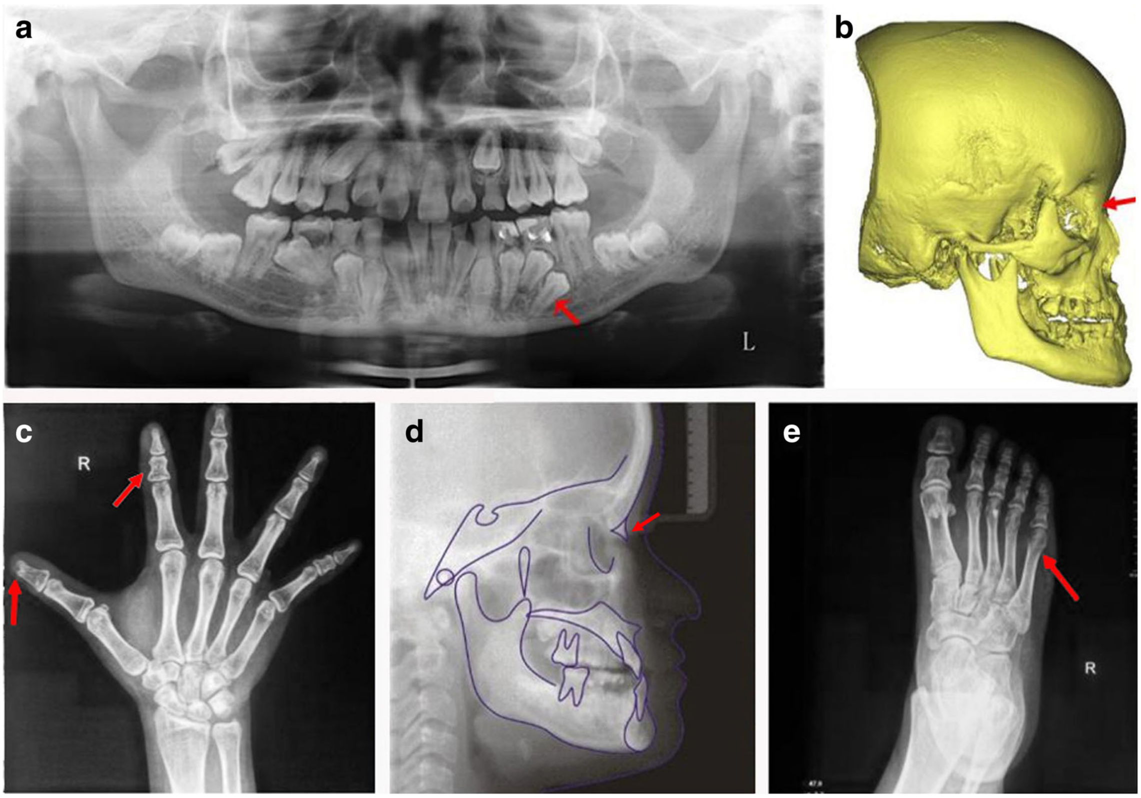

Fig. 2 Radiological findings in the proband. **a** Panoramic radiograph showing many retained deciduous teeth and unerupted permanent teeth and one supernumerary tooth between the left second premolar and first molar in the mandible (indicated by red arrow). **b** 3D reconstruction of skull showing prominent forehead and no nasal bone (indicated by red arrow). **c**, **e** Hand and foot radiograph showing hypoplasia of distal phalanges (indicated by red arrows in **c**) and crooked metatarsal (indicated by red arrow in **e**). **d** Cephalometric X-ray showing maxillary dysplasia, mandibular prognathism, and no nasal bone (indicated by red arrow)

Table 2 Cephalometric analysis

Measurement	Proband	Standard
SNA	95°	83.13 ± 3.60°
SNB	97°	79.65 ± 3.20°
ANB	−2°	3.48 ± 1.69°
Ptm-A	45 mm	44.89 ± 2.76 mm
Ptm-S	15 mm	17.70 ± 2.24 mm
PP-FH	5°	4.48 ± 3.10°
PP-GogGn	11°	21.13 ± 4.15°
OP-SN	7.5°	19.41 ± 3.85°
Go-Pg	68 mm	72.53 ± 4.40 mm
Go-Co	52 mm	55.85 ± 3.96 mm
Pcd-S	8 mm	17.48 ± 2.62 mm
SN-MP	17°	32.85 ± 4.21°
Y-axis	53°	63.54 ± 3.23°
NBa-PtGn	71°	87.76 ± 3.46°
ANS-Me	49 mm	61.09 ± 3.36 mm
S-Go	70 mm	75.26 ± 4.70 mm
S-Go/N-Me	75.83%	65.85 ± 3.83%
ANS-Me/N-Me	53.33%	53.32 ± 1.84%
U1-L1	152°	126.96 ± 8.54°
U1-SN	114°	75.38 ± 6.02°
U1-NA	0 mm	4.05 ± 2.32 mm
U1-NA°	12°	21.49 ± 5.92°
L1-NB	− 3 mm	5.69 ± 2.05 mm
L1-NB°	10°	28.07 ± 5.58°
Wits	− 7.7 mm	0 mm
FMIA	87°	57.00 ± 6.79°

containing the extracted metabolites were transferred to new tubes and stored at − 80 °C until further analysis.

LC-MS/MS analysis of metabolites and data analysis

Metabolites were analyzed using an LC-MS/MS system equipped with Shimadzu LC20A (Shimadzu, Japan) coupled with Qtrap 5500 (ABSCIEX, USA). LC-MS/MS analysis was performed by multiple reaction monitoring (MRM) using Analyst v1.6.1 (AB SCIEX, Framingham, MA, USA) software. Two injections were conducted, one on positive and one on negative mode. Ten microliters of the respective extracts were injected by a PAL CTC autosampler into a 250 × 2 mm, 5 μm Luna NH2 aminopropyl HPLC column (Phenomenex, Torrance, CA, USA) held at 25 °C for chromatographic separation. A total of 320 metabolites were analyzed. Metabolomic data were log2-transformed and analyzed by multivariate partial least-square discriminant analysis (PLS-DA) in MetaboAnalyst. Metabolites with variable importance in projection (VIP) scores greater than 1.5 were considered significant [19]. Metabolic pathways were analyzed in metaboanalyst and reconfirmed using KEGG pathway analysis.

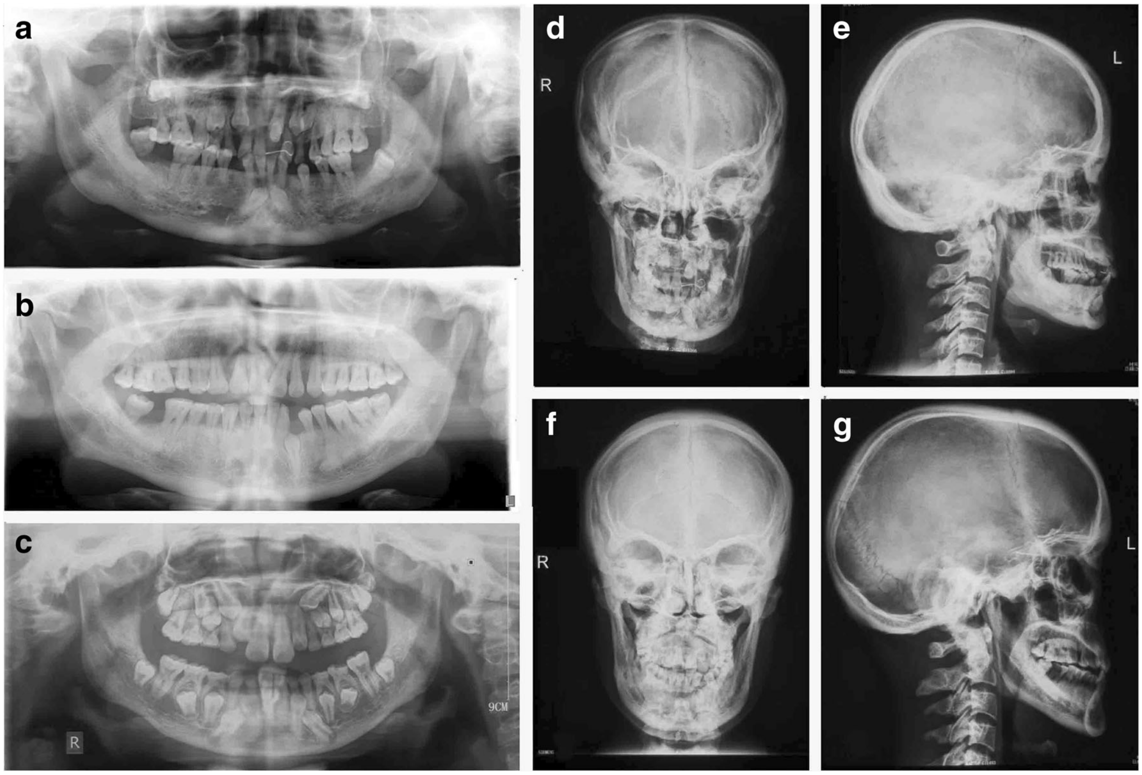

Fig. 3 Radiological findings in CCD-affected relatives of the proband. **a** Panoramic radiograph of the proband's mother showing multiple unerupted teeth and one supernumerary tooth. **b** Panoramic radiograph of the proband's uncle showing one unerupted tooth. **c** Panoramic radiograph of the proband's cousin shows multiple retained deciduous teeth and unerupted permanent teeth. **d**, **e** Anteroposterior and lateral view of the skull of the proband's mother demonstrating frontal suture, several impacted teeth, and absence of nose bone. **f, g** Anteroposterior and lateral view of the skull of proband's uncle showing interparietal suture and impacted tooth

Results

Clinical findings of CCD patients

The pedigree for the CCD family is shown in Fig. 1. The initial 24-year-old proband (Fig. 1, black arrow) presented with a short stature (height 148 cm, body weight 42 kg), midface hypoplasia, anterior cross-bite, widened eye distance, depressed nasal bridge, widened nose, and short hands and feet. Radiological findings showed many retained deciduous teeth and unerupted permanent teeth and one supernumerary tooth (Fig. 2a, red arrow) between the left second premolar and first molar in the mandible. The nasal bone was almost invisible on 3D reconstruction (Fig. 2b, red arrow) and cephalometric film (Fig. 2d, red arrow). The radiological examination of the hands and feet revealed hypoplastic distal phalanges (Fig. 2c, red arrows) and crooked metatarsals (Fig. 2e, red arrow). Cephalometric analysis revealed that the proband had a Class III skeletal deformity and an abnormal SN plane due to abnormal cranial development (Table 2). Symptoms similar to those of the proband were found in her mother, grandmother, uncle, and cousin (Fig. 3, Table 3).

Mutational analysis of *RUNX2* and protein structure predictions

Because CCD has previously been found to be associated with *RUNX2* mutations, it was likely that the patients in our

Table 3 Clinical and genetic findings in affected patients

Patients	Age	Sex	Stature	Affected bone	Delayed eruption teeth	Supernumerary teeth	Nucleotide change	Exon	Domain
Proband	25	F	148 cm	Hand/maxilla	18	1	c.1061insT	8	PST
Grandmother	71	F	155 cm	–	–	–	c.1061insT	8	PST
Mother	48	F	150 cm	Hand/maxilla	9	1	c.1061insT	8	PST
Uncle	40	M	165 cm	Hand/maxilla	1	0	c.1061insT	8	PST
Cousin	14	M	150 cm	–	18	0	c.1061insT	8	PST

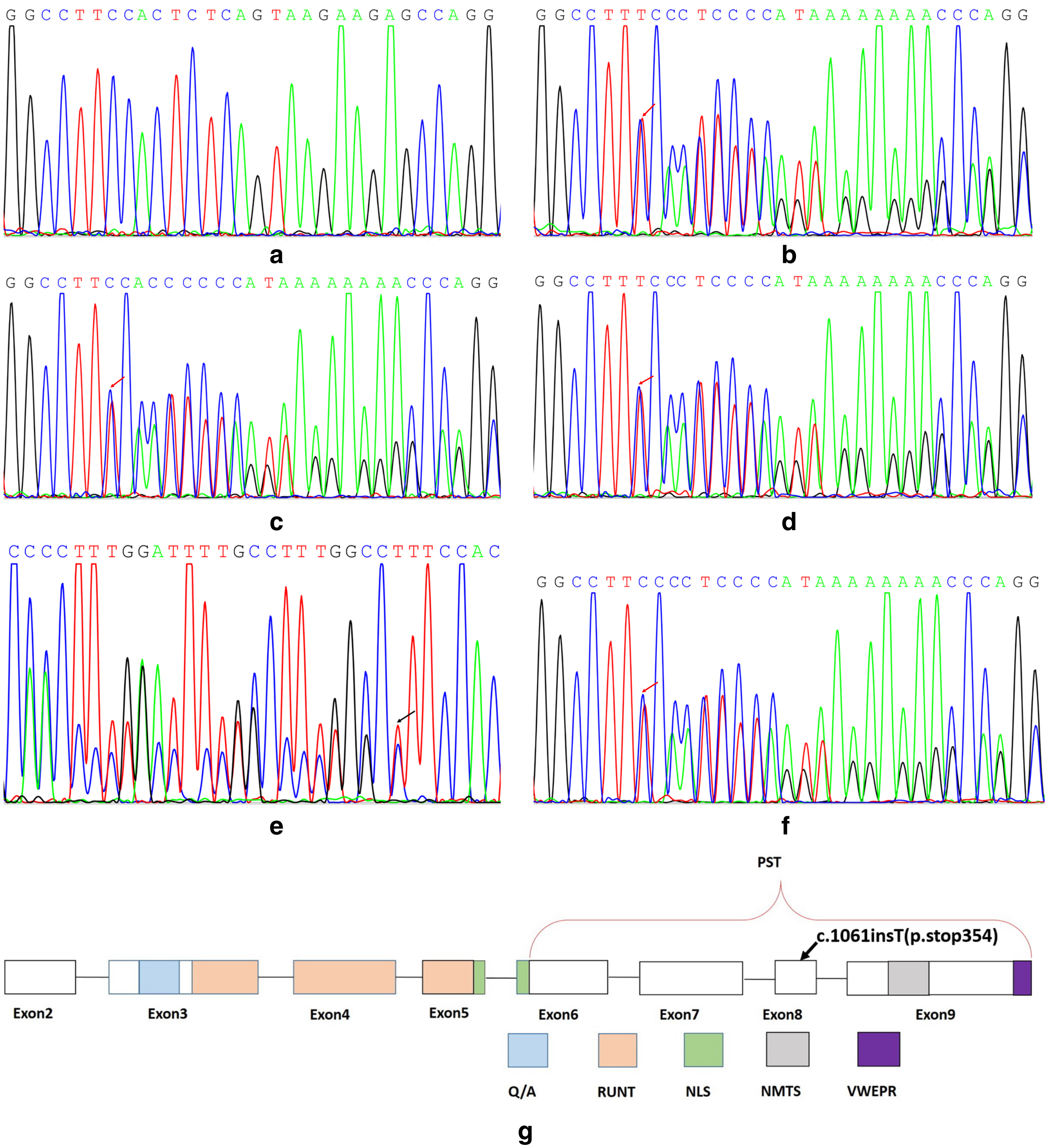

Fig. 4 DNA-sequence electropherogram of the family with CCD patients and normal people; arrows indicate the mutations in the sequence. **a** Wild-type sequence in a normal individual; **b** proband's grandmother (c.1061insT); **c** proband's mother (c.1061insT); **d** proband (c.1061insT); **e** proband's uncle; **f** proband's cousin (c.1061insT). **g** Schematic diagram of the *RUNX2* gene and position of the new mutation (arrow)

family also carried a mutation in this gene. Hence, we analyzed the genomic sequence of all eight coding exons after PCR amplification. DNA-sequence electropherograms of normal individuals (Fig. 4a) and the CCD patients (Fig. 4b–f) show that the proband, her mother, grandmother, uncle, and cousin all carried an insertion of a T at position 1061 in exon 8 of *RUNX2*. This mutation has not been reported previously and is not present in unaffected family members, suggesting that the sequence alteration does not represent a gene polymorphism. Notably, the insertion

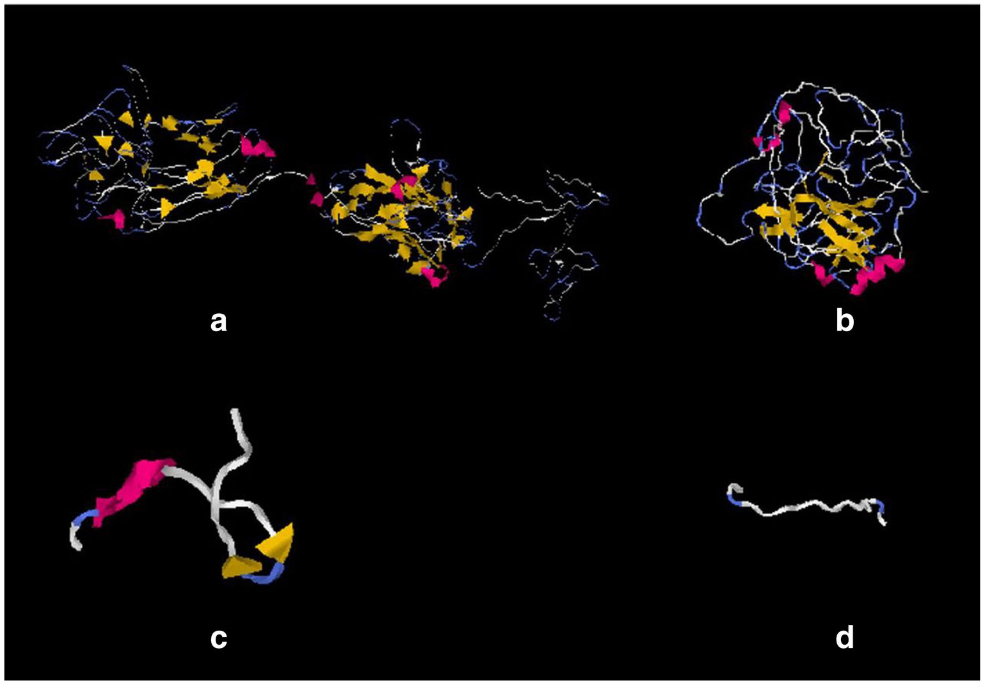

Fig. 5 Structure of normal and mutant protein predicted by I-TASSER. **a** Predicted structure of normal RUNX2; **b** mutant RUNX2; **c** predicted structure of normal isolated exon 8; **d** predicted structure of mutant exon 8. Red, α-helices; yellow, β-strands; blue, β-turns

would result in a frame shift in the coding region and a premature stop at residue 354, leading to a truncated protein lacking 164 carboxyl terminal amino acids. Such a truncated protein would likely have an altered function as the truncation affects the functionally important PST domain. This interpretation is supported by 3D protein structure predictions obtained using RosMol version 2.7.5.2. The predictions indicate that the mutant protein would lose most of the β-strands and H-bonds (Fig. 5, Table 4), likely leading to alterations in the regulation of its downstream target genes and corresponding signaling pathways. Alternatively, however, the mutation may also affect the stability of the protein or lead to an overall reduction in protein expression because the premature stop codon is located in the penultimate exon, potentially subjecting the corresponding mRNA to nonsense-mediated decay. Additionally, exon 8 may be alternatively spliced out, leading to a protein with an internal deletion.

Table 4 Prediction of protein secondary structure change

	Number of H-bonds	Number of α-helices	Number of β-strands	Number of β-turns
Exon 8 mutation	7	0	0	2
Exon 8 normal	13	1	2	2
RUNX2 mutation	144	4	14	57
RUNX2 normal	234	5	45	70

Metabolic analysis

To correlate the novel *RUNX2* mutation with metabolic changes, we then performed a broad metabolomics profiling in patient plasma. Over 320 metabolites in major human metabolic pathways were detected. The top 30 significantly changed metabolites ranked according to VIP scores are shown in Fig. 6a, b, and c. PLS-DA analysis revealed that three metabolites among the 30 analyzed were significantly increased in CCD patients compared to normal controls. They included serotonin, ceramide (18:1/23:0), and phosphatidylinositol (PI, 36:0), while the other 27 were sharply reduced, with the top decrease observed in gluconolactone, followed by phosphatidylserine (34:1) and L-glutamic acid (Fig. 6b). Biochemical pathway analysis identified 13 metabolic pathways with significant changes, with amino acid metabolism, glycolysis, and TCA cycle being prominently altered in CCD patients. Detailed information on these pathways is shown in Table 5. Our results showed that aminoacyl-tRNA was significantly down-regulated in the

Fig. 6 The metabolomic analysis of CCD patients and normal controls. **a** PLS-DA analysis revealed significant metabolic differences between CCD patients and normal controls. **b** Targeted metabolites (VIP scores ≥ 1.5 were considered statistically significant). Among the 30 metabolites analyzed, three were significantly increased, while the other 27 were sharply reduced. **c** Major metabolic pathways altered in CCD patients include amino acid metabolism, glycolysis metabolism, TCA cycle, and others as indicated. **d**, **e** The downregulation of amino acid and aminoacyl-tRNA biosynthesis in CCD associated with RUNX2 mutation. Numbers in red fonts indicate the peak area ratio of CCD patients/normal control

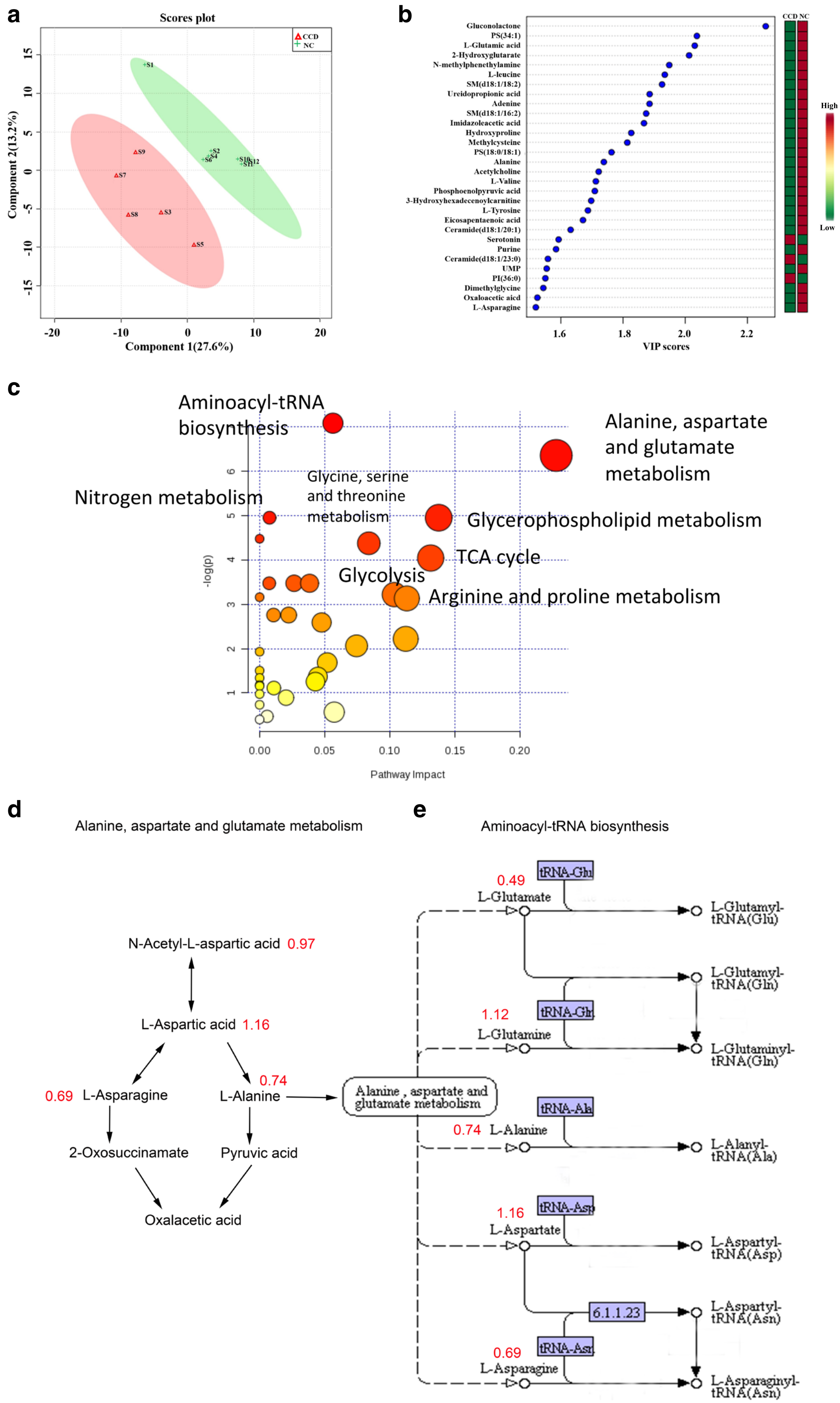
a
Scores plot
CCD
NC
S1
S2
S4
S6
S10
S11
S12
S9
S7
S8
S3
S5
Component 2(13.2%)
Component 1(27.6%)
-20
-10
0
10
20
15
10
5
0
-5
-10
-15
b
Gluconolactone
PS(34:1)
L-Glutamic acid
2-Hydroxyglutarate
N-methylphenethylamine
L-leucine
SM(d18:1/18:2)
Ureidopropionic acid
Adenine
SM(d18:1/16:2)
Imidazoleacetic acid
Hydroxyproline
Methylcysteine
PS(18:0/18:1)
Alanine
Acetylcholine
L-Valine
Phosphoenolpyruvic acid
3-Hydroxyhexadecenoylcarnitine
L-Tyrosine
Eicosapentaenoic acid
Ceramide(d18:1/20:1)
Serotonin
Purine
Ceramide(d18:1/23:0)
UMP
PI(36:0)
Dimethylglycine
Oxaloacetic aicd
L-Asparagine
1.6
1.8
2.0
2.2
VIP scores
CCD NC
High
Low
c
Aminoacyl-tRNA biosynthesis
Alanine, aspartate and glutamate metabolism
Glycine, serine and threonine metabolism
Nitrogen metabolism
Glycerophospholipid metabolism
TCA cycle
Glycolysis
Arginine and proline metabolism
-log(p)
Pathway Impact
0.00
0.05
0.10
0.15
0.20
1
2
3
4
5
6
d
Alanine, aspartate and glutamate metabolism
N-Acetyl-L-aspartic acid 0.97
L-Aspartic acid 1.16
0.69 L-Asparagine
0.74 L-Alanine
2-Oxosuccinamate
Pyruvic acid
Oxalacetic acid
e
Aminoacyl-tRNA biosynthesis
tRNA-Glu
0.49 L-Glutamate
L-Glutamyl-tRNA(Glu)
L-Glutamyl-tRNA(Gln)
tRNA-Gln
1.12 L-Glutamine
L-Glutaminyl-tRNA(Gln)
Alanine , aspartate and glutamate metabolism
tRNA-Ala
0.74 L-Alanine
L-Alanyl-tRNA(Ala)
tRNA-Asp
1.16 L-Aspartate
L-Aspartyl-tRNA(Asp)
6.1.1.23
L-Aspartyl-tRNA(Asn)
tRNA-Asn
0.69 L-Asparagine
L-Asparaginyl-tRNA(Asn)

Table 5 Pathways analysis between CCD and normal controls

Pathway name	Total	Hits	p value	-log(p)	Holm p	FDR	Impact
Aminoacyl-tRNA biosynthesis	75	5	0.001	7.085	0.067	0.067	0.056
Alanine, aspartate, and glutamate metabolism	24	3	0.002	6.356	0.137	0.069	0.228
Nitrogen metabolism	39	3	0.007	4.952	0.552	0.141	0.008
Glycerophospholipid metabolism	39	3	0.007	4.952	0.552	0.141	0.138
Cyanoamino acid metabolism	16	2	0.011	4.477	0.864	0.168	0.000
Glycine, serine, and threonine metabolism	48	3	0.013	4.375	0.944	0.168	0.084
Citrate cycle (TCA cycle)	20	2	0.018	4.043	1.000	0.201	0.131
Phenylalanine, tyrosine, and tryptophan biosynthesis	27	2	0.031	3.473	1.000	0.248	0.007
Valine, leucine, and isoleucine biosynthesis	27	2	0.031	3.473	1.000	0.248	0.027
Pantothenate and CoA biosynthesis	27	2	0.031	3.473	1.000	0.248	0.038
Glycolysis or gluconeogenesis	31	2	0.040	3.217	1.000	0.269	0.104
Pyruvate metabolism	32	2	0.042	3.159	1.000	0.269	0.000
Arginine and proline metabolism	77	3	0.044	3.131	1.000	0.269	0.113

CCD group, indicating a disruption of protein synthesis in individuals with the *RUNX2* mutation (Fig. 6d). This might be due to the decrease of amino acids in CCD patients as shown in Fig. 6e.

Discussion

We provide the first metabolomics profiling in a familial case of CCD with a novel mutation in *RUNX2* (c.1061insT). We find that 30 metabolites in 13 metabolic pathways were significantly changed in CCD patients. Both genomic and metabolic analyses may provide important information about CCD and novel insights for diagnostics and potentially therapeutics.

Hypoplastic clavicles, delayed closure of fontanelles, and delayed eruption of permanent teeth are the main characteristics of CCD. Nevertheless, previous studies have described patients that exhibit a family history typical for CCD but lack some of the clinical characteristics normally observed in CCD patients [2]. It was suggested, therefore, that CCD should still be considered in patients who present with dental abnormalities such as delayed tooth eruption and supernumerary teeth, especially when they display a family history [20]. Therefore, in such patients, the diagnosis of CCD should be confirmed by a more detailed examination including gene mutational analyses.

In 1997, Mundlos et al. first established that heterozygosity for mutations in *RUNX2* were responsible for CCD [3]. Thus far, more than 100 distinct mutations in *RUNX2* have been detected. The mutations are located throughout the gene, but most are clustered in the Runt domain, with fewer in the PST and the Q/A region [21]. Nevertheless, mutations in *RUNX2* could only be detected in 60–70% of CCD patients. Thirteen percent of patients have other genetic abnormalities including large chromosomal deletions or translocations and intragenic microdeletions, but the genetic etiologies in the remaining patients remain unknown [22, 23].

The new mutation in exon 8 that causes a translational frame shift and predicts a loss of the carboxyl terminus of RUNX2 may affect the stability and function of the protein and may hence cause functional haploinsufficiency of RUNX2. Bufalino et al. considered that mutations affecting the runt domain are associated with severe dental problems including failure of eruption of multiple teeth and the presence of supernumerary teeth, while mutations outside the Runt domain show only mild dental phenotypes [24]. Ankur Singh showed that a milder dental abnormality and normal clavicles were associated with a mutation in the Q/A domain [25]. Here, we found that typical dental abnormalities associated with a mutation in the PST domain. This suggests that it is not yet possible to clearly correlate a given genotype with a specific phenotype.

RUNX2 plays an important role in bone formation, which is a dynamic process regulated by bone metabolism that itself is an important aspect of the metabolism of the entire body. One may therefore expect that there are metabolic differences between normal individuals and patients with CCD, regardless of which gene mutation is responsible for the disorder. Indeed, we here identified 30 metabolites in 13 metabolic pathways that were changed in our CCD patients. By detecting small molecules and identifying alterations in metabolic processes, metabolomic analysis has been shown to be a convenient, sensitive, and reliable method in the diagnosis of diseases [25]. An increasing number of studies have revealed a role for RUNX2 in metabolic processes [26–28]. Recent studies focusing on bone metabolism and tumor metastasis have shown that RUNX2 can regulate the metabolism of glycolysis, glutamine, sterol/steroid, insulin, and lipids [14, 29–32]. To our knowledge, the present study is the first to demonstrate metabolic changes in CCD patients with a *RUNX2* mutation. It is plausible that alterations in RUNX2 protein such as those brought about by the lack of part of the PST transcriptional activation domain would lead to a dysregulation of the expression of target genes involved in cell metabolism. Although we could not thus far demonstrate significant changes in potential *RUNX2* target genes affecting metabolism, such as GLUT1, SIRT6, SGPP1, or P53, we believe that more detailed studies of the correlation between disease-associated *RUNX2* mutations and metabolic changes remain a highly attractive approach to gain deeper insights into pathogenesis and ultimately provide means toward rational therapies.

The metabolic abnormalities we describe here were observed in adult CCD patients, indicating that metabolic changes persist long after the disease processes first appear during development. The presence of a mutation in a transcription factor gene in our patients was clearly associated with metabolic changes. This strongly suggests a causal relationship between genotype and phenotype. Further studies will show whether the metabolic changes observed in our CCD patients are also observed in patients with other *RUNX2* mutations or even other genomic alterations. The analysis of metabolic changes in these genetic disorders may become an important part to aid in their differential diagnosis.

Conclusions

The results obtained in the current study contribute to the understanding of the correlation between clinical features, mutations, and metabolic changes in affected members of a CCD family. We anticipate that such correlative studies will become more important not only for basic biomedical research but also for clinical diagnostics and, potentially, therapeutics.

Funding The work was supported by the Southern Medical University (grants PY2017N036); National Natural Science Foundation of China (grants 81571020 and 81771124); Natural Science Foundation of Guangdong Province (grants 2015A030313179).

Compliance with ethical standards

Conflict of interest Z.Z. declares that he has no conflict of interest. K.L. declares that he has no conflict of interest. M.Y. declares that he has no conflict of interest. Q.L. declares that he has no conflict of interest. J.L. declares that he has no conflict of interest. P.Z. declares that he has no conflict of interest. Y.X. declares that he has no conflict of interest.

Ethical approval All procedures performed in our study involving human participants were in accordance with the ethical standards of the institutional research committee and with the 1964 Helsinki declaration and its later amendments or comparable ethical standards.

Informed consent Informed consent was obtained from all individual participants included in the study.

References

1. Cooper SC, Flaitz CM, Johnston DA, Lee B, Hecht JT (2001) A natural history of cleidocranial dysplasia. Am J Med Genet 104(1):1–6
2. Mundlos S (1999) Cleidocranial dysplasia: clinical and molecular genetics. J Med Genet 36(3):177–182
3. Mundlos S, Otto F, Mundlos C, Mulliken JB, Aylsworth AS, Albright S, Lindhout D, Cole WG, Henn W, Knoll JH, Owen MJ, Mertelsmann R, Zabel BU, Olsen BR (1997) Mutations involving the transcription factor CBFA1 cause cleidocranial dysplasia. Cell 89(5):773–779
4. Lee B, Thirunavukkarasu K, Zhou L, Pastore L, Baldini A, Hecht J, Geoffroy V, Ducy P, Karsenty G (1997) Missense mutations abolishing DNA binding of the osteoblast-specific transcription factor OSF2/CBFA1 in cleidocranial dysplasia. Nat Genet 16(3): 307–310
5. Ducy P, Zhang R, Geoffroy V, Ridall AL, Karsenty G (1997) Osf2/Cbfa1, a transcriptional activator of osteoblast differentiation. Cell 89(5):747–754
6. Yoshida CA, Yamamoto H, Fujita T, Furuichi T, Ito K, Inoue K, Yamana K, Zanma A, Takada K, Ito Y, Komori T (2004) Runx2 and Runx3 are essential for chondrocyte maturation, and Runx2 regulates limb growth through induction of Indian hedgehog. Genes Dev 18(8):952–963
7. Li Y, Xiao Z (2007) Advances in Runx2 regulation and its isoforms. Med Hypotheses 68(1):169–175
8. Thirunavukkarasu K, Mahajan M, McLarren KW, Stifani S, Karsenty G (1998) Two domains unique to osteoblast-specific transcription factor Osf2/Cbfa1 contribute to its transactivation function and its inability to heterodimerize with Cbfβ. Mol Cell Biol 18(7):4197–4208
9. Zhang YW, Yasui N, Ito K, Huang G, Fujii M, Hanai J, Nogami H, Ochi T, Miyazono K, Ito Y (2000) A RUNX2/PEBP2αA/CBFA1 mutation displaying impaired transactivation and Smad interaction in cleidocranial dysplasia. Proc Natl Acad Sci U S A 97(19):10549–10554
10. Afzal F, Pratap J, Ito K, Ito Y, Stein JL, van Wijnen AJ, Stein GS, Lian JB, Javed A (2005) Smad function and intranuclear targeting share a Runx2 motif required for osteogenic lineage induction and BMP2 responsive transcription. J Cell Physiol 204(1):63–72
11. Zelzer E, Glotzer DJ, Hartmann C, Thomas D, Fukai N, Soker S, Olsen BR (2001) Tissue specific regulation of VEGF expression during bone development requires Cbfa1/Runx2. Mech Dev 106(1–2):97–106
12. Zaidi SK, Pande S, Pratap J, Gaur T, Grigoriu S, Ali SA, Stein JL, Lian JB, van Wijnen AJ, Stein GS (2007) Runx2 deficiency and defective subnuclear targeting bypass senescence to promote immortalization and tumorigenic potential. Proc Natl Acad Sci U S A 104(50):19861–19866
13. Mak IW, Cowan RW, Popovic S, Colterjohn N, Singh G, Ghert M (2009) Upregulation of MMP-13 via Runx2 in the stromal cell of giant cell tumor of bone. Bone 45(2):377–386
14. Teplyuk NM, Zhang Y, Lou Y, Hawse JR, Hassan MQ, Teplyuk VI, Pratap J, Galindo M, Stein JL, Stein GS, Lian JB, van Wijnen AJ (2009) The osteogenic transcription factor runx2 controls genes involved in sterol/steroid metabolism, including CYP11A1 in osteoblasts. Mol Endocrinol 23(6):849–861
15. Sawai CM, Sisirak V, Ghosh HS, Hou EZ, Ceribelli M, Staudt LM, Reizis B (2013) Transcription factor Runx2 controls the development and migration of plasmacytoid dendritic cells. J Exp Med 210(11):2151–2159
16. Stein GS, Lian JB, van Wijnen AJ, Stein JL, Montecino M, Javed A, Zaidi SK, Young DW, Choi JY, Pockwinse SM (2004) Runx2 control of organization, assembly and activity of the regulatory

machinery for skeletal gene expression. Oncogene 23(24):4315–4329

17. Lee KS, Kim HJ, Li QL, Chi XZ, Ueta C, Komori T, Wozney JM, Kim EG, Choi JY, Ryoo HM, Bae SC (2000) Runx2 is a common target of transforming growth factor β1 and bone morphogenetic protein 2, and cooperation between Runx2 and Smad5 induces osteoblast-specific gene expression in the pluripotent mesenchymal precursor cell line C2C12. Mol Cell Biol 20(23):8783–8792
18. Putri SP, Nakayama Y, Matsuda F, Uchikata T, Kobayashi S, Matsubara A, Fukusaki E (2013) Current metabolomics, practical applications. J Biosci Bioeng 115(6):579–589
19. Yuan M, Breitkopf SB, Yang X, Asara JM (2012) A positive/negative ion-switching, targeted mass spectrometry-based metabolomics platform for bodily fluids, cells, and fresh and fixed tissue. Nat Protoc 7(5):872–881
20. Zhang C, Zheng S, Wang Y, Zhao Y, Zhu J, Ge L (2010) Mutational analysis of RUNX2 gene in Chinese patients with cleidocranial dysplasia. Mutagenesis 25(6):589–594
21. Wang S, Zhang S, Wang Y, Chen Y, Zhou L (2013) Cleidocranial dysplasia syndrome, clinical characteristics and mutation study of a Chinese family. Int J Clin Exp Med 6(10):900–907
22. Otto F, Kanegane H, Mundlos S (2002) Mutations in the RUNX2 gene in patients with cleidocranial dysplasia. Hum Mutat 19(1):209–216
23. Ott CE, Leschik G, Trotier F, Brueton L, Brunner HG, Brussel W, Guillen-Navarro E, Haase C, Kohlhase J, Kotzot D, Lane A, Lee-Kirsch MA, Morlot S, Simon ME, Steichen-Gersdorf E, Tegay DH, Peters H, Mundlos S, Klopocki E (2010) Deletions of the RUNX2 gene are present in about 10% of individuals with cleidocranial dysplasia. Hum Mutat 31(8):15871593
24. Baumert U, Golan I, Redlich M, Aknin JJ, Muessig D (2005) Cleidocranial dysplasia, molecular genetic analysis and phenotypic-based description of a middle European patient group. Am J Med Genet 139((2):78–85
25. Bufalino A, Paranaíba LM, Gouvêa AF, Gueiros LA, Martelli-Júnior H, Junior JJ, Lopes MA, Graner E, De Almeida OP, Vargas PA, Coletta RD (2012) Cleidocranial dysplasia, oral features and genetic analysis of 11 patients. Oral Dis 18(2):184–190
26. Singh A, Goswami M, Pradhan G, Han MS, Choi JY, Kapoor S (2015) Cleidocranial dysplasia with normal clavicles, a report of a novel genotype and a review of seven previous cases. Mol Syndromol 6(2):83–86
27. Madsen R, Lundstedt T, Trygg J (2010) Chemometrics in metabolomics—a review in human disease diagnosis. Anal Chim Acta 659(1–2):23–33
28. Chang DJ, Ji C, Kim KK, Casinghino S, McCarthy TL, Centrella M (1998) Reduction in transforming growth factor b receptor I expression and transcription factor CBFa1 on bone cells by glucocorticoid. J Biol Chem 273(9):4892–4896
29. Baniwal SK, Khalid O, Gabet Y, Shah RR, Purcell DJ, Mav D, Kohn-Gabet AE, Shi Y, Coetzee GA, Frenkel B (2010) Runx2 transcriptome of prostate cancer cells, insights into invasiveness and bone metastasis. Mol Cancer 9:258
30. Kilbey A, Terry A, Jenkins A, Borland G, Zhang Q, Wakelam MJ, Cameron ER, Neil JC (2010) Runx regulation of sphingolipid metabolism and survival signaling. Cancer Res 70(14):5860–5869
31. Choe M, Brusgard JL, Chumsri S, Bhandary L, Zhao XF, Lu S, Goloubeva OG, Polster BM, Fiskum GM, Girnun GD, Kim MS, Passaniti A (2015) The RUNX2 transcription factor negatively regulates SIRT6 expression to Alter glucose metabolism in breast Cancer cells. J Cell Biochem 116(10):2210–2226
32. Adhami M, Ghori-Javed FY, Chen H, Gutierrez SE, Javed A (2011) Runx2 regulates the gene network associated with insulin signaling and energy homeostasis. Cells Tissues Organs 194(2–4):232–237